Supplemental Materials

Beneficial microbes mitigate molecular stress responses and accelerate developmental pathways in host animals during spaceflight

Eric J. Koch[1#], Ana Conesa[2], Timothy J. Garrett[3], Rachel Ormsby[4], Ryan Bohl[4], David Reed[4], Jamie S. Foster[1]*

[1]Department of Microbiology and Cell Science, Space Life Science Lab, University of Florida, Merritt Island, FL 32953, USA

[2]Spanish National Research Council, Institute for Integrative Systems Biology, Valencia, Spain

[3]Department of Pathology, Immunology and Laboratory Medicine, College of Medicine, University of Florida, Gainesville, FL 32611, USA

[4]Redwire Space Technologies, Inc., Greenville, IN 47124

*Corresponding author: jfoster@ufl.edu; ORCID: 0000-0001-8603-4006

#Current location: Observatoire Océanologique de Banyuls-sur-mer, Banyuls-sur-mer, France

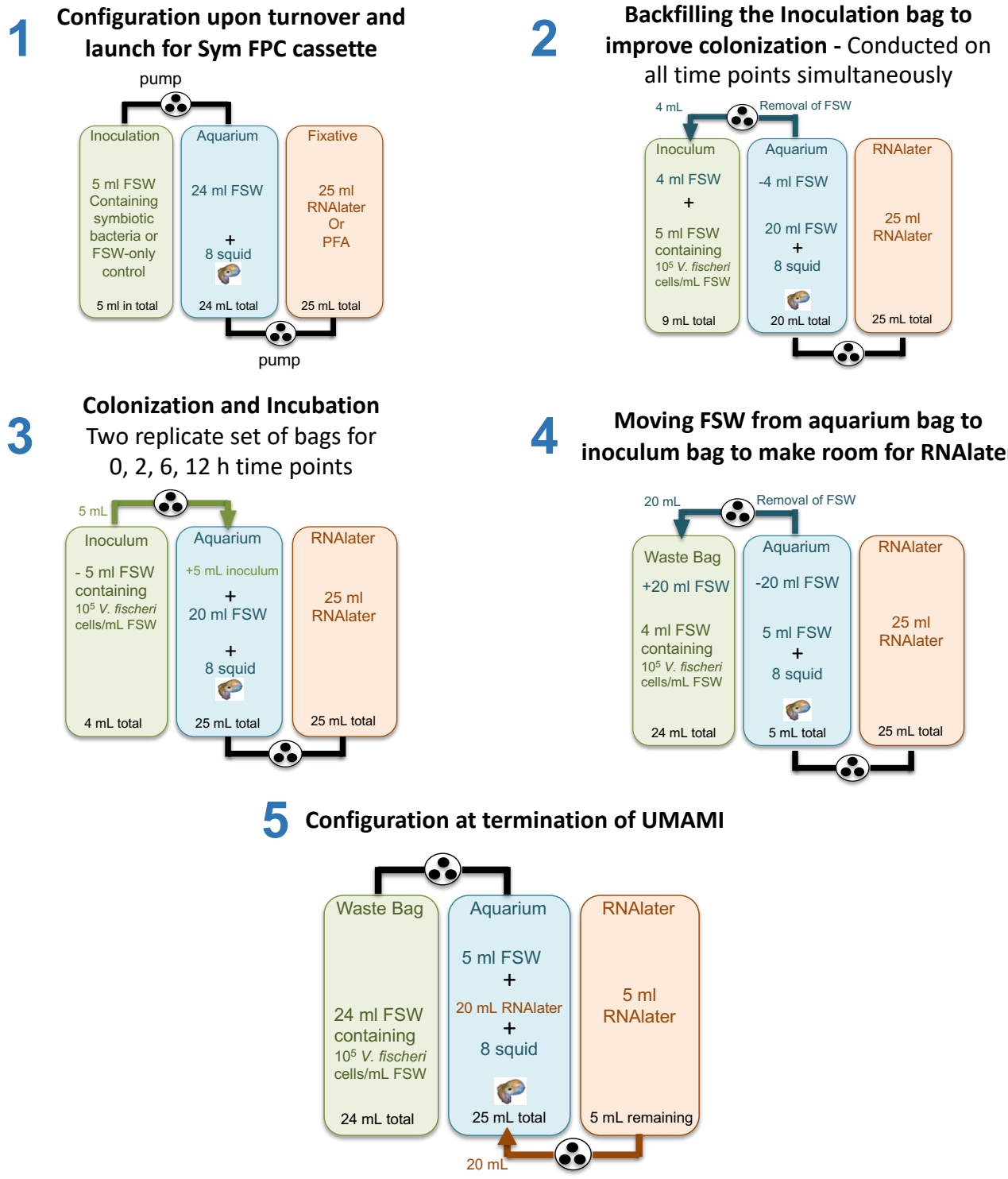

Supplemental Fig. S1. Overview of the experimental protocol and loop design for the UMAMI flight experiment. A total of 16 loops each containing an Inoculation, Aquarium and Fixation bag were housed within two Fluid Processing Cassettes. The configuration of the symbiotic (Sym) loop design is shown with the following steps: 1) configuration at the time of launch; 2) initiation of the experiment by backfilling the inoculation bag to facilitate mixing of the symbiont and make room in the aquarium bag for inoculation; 3) Colonization times for the incubation of either symbiont; 4) After incubation, fluid from aquarium back is moved back into Inoculation bag (now labeled Waste bag) to make room for RNALater; and 5) configuration of RNALater preserved squid. Note for the aposymbiotic controls, which were housed in a separate FPC, only filtered sea water (FSW) was added during the "inoculation" stages.

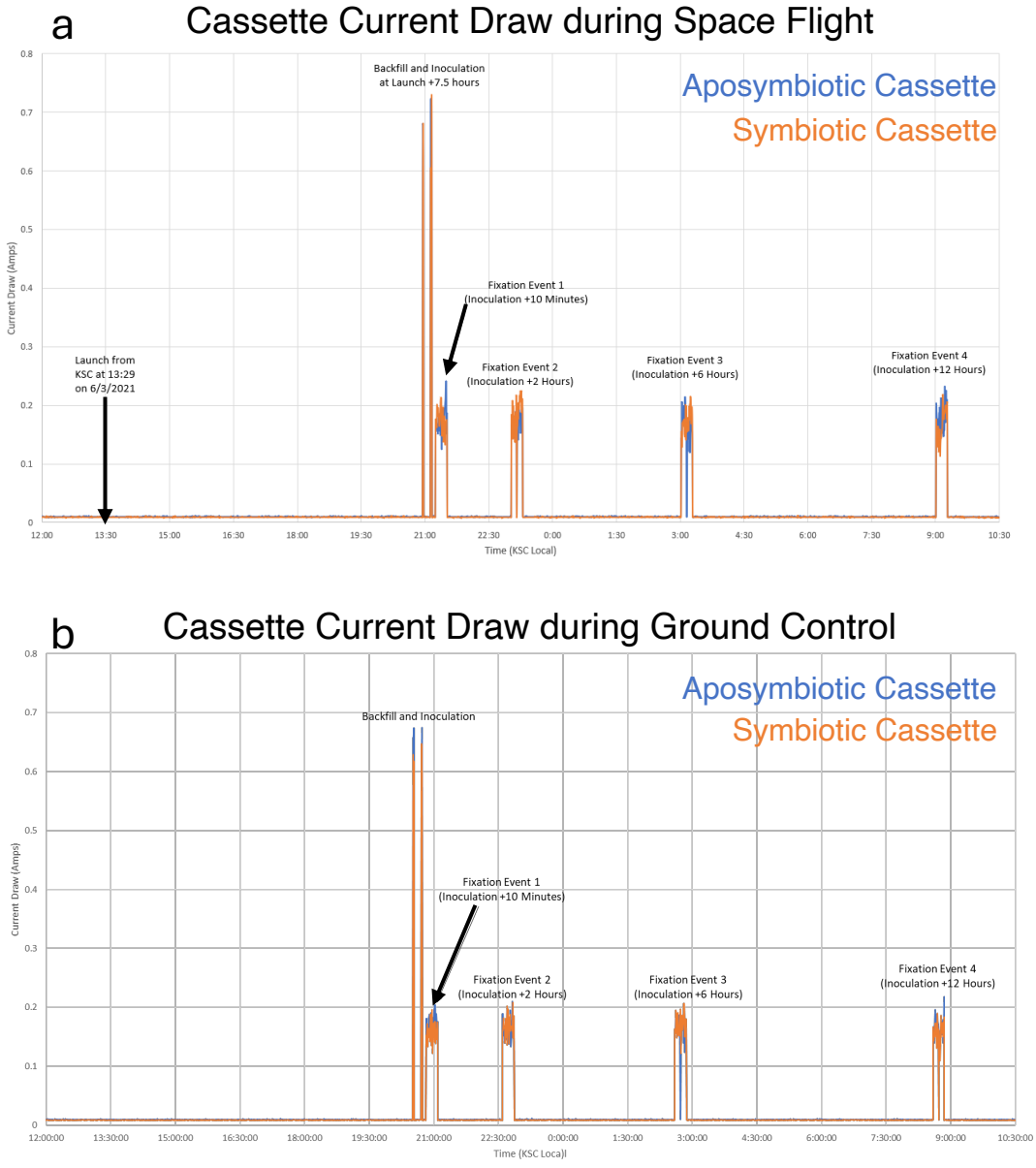

Supplemental Fig. S2. Overview of the UMAMI operations and electrical current draws of the two fluid processing cassettes within the ADvanced Space Experiment Processor (ADSEP) facility. Results suggest the UMAMI experiment was successfully completed, and all inoculation, incubation, and fixation termination events occurred as planned during both the spaceflight (**a**) and ground controls (**b**). The ADSEP facility monitored the current draw of both the aposymbiotic (blue) and symbiotic (orange) fluid processing cassette showing spikes when motors were activated, and the power draws matched the expected UMAMI timeline indicating the flight hardware operated as expected.

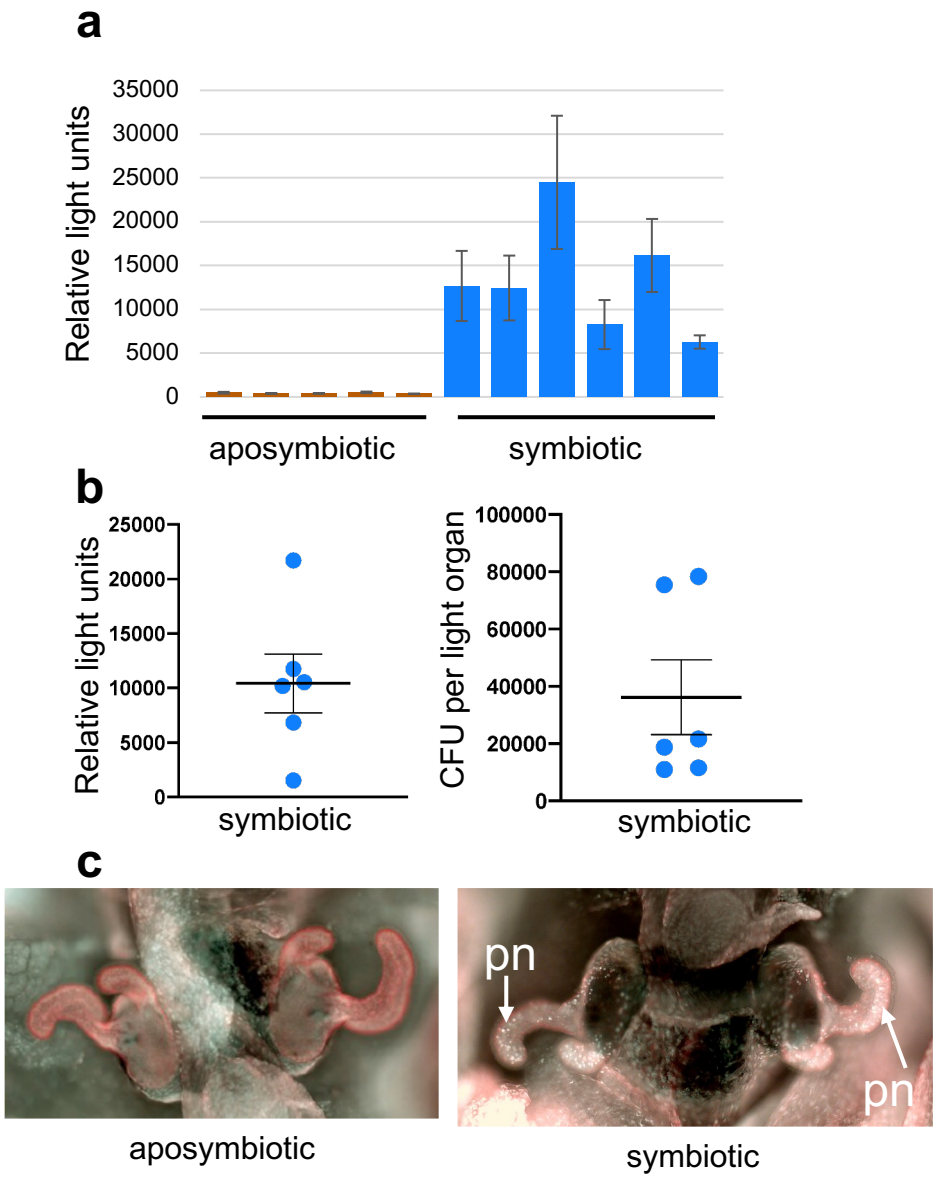

Supplemental Fig. S3. Confirmation of light organ colonization by *Vibrio fischeri* during the Equipment Verification Testing (EVT) of the the ADvanced Science Experiment Processor (ADSEP) hardware. The experimental protocol was conducted in the ADSEP hardware and stopped after colonization and prior to RNALater fixation to ensure effective colonization of the animals by the symbiotic bacteria. **(a)** At 16 h post-inoculation, animals were removed from their aquarium bags and were individually assessed for luminescence. All animals exposed to *V. fischeri* exhibited high luminescence compared to the aposymbiotic controls suggesting the animals were effectively colonized in the ADSEP hardware. (b) Further characterization of symbiotic light organs through both luminescence readings and subsequent plating of the light organ indicated colony forming units (CFUs) indicated the presence of *V. fischeri* in the symbiotic light organs. (c) Lastly, well-established developmental markers such as the onset of *V. fischeri*-induced apoptosis in the superficial ciliated epithelial cells of the light organ were monitored. After 16 h post-inoculation, pronounced pycnotic nuclei (arrows) were visible in symbiotic animals stained with acridine orange compared to aposymbiotic controls. Together, the luminescence, cell plating, and apoptotic cell death suggested that normal colonization occurred in the host animals within the ADSEP flight hardware.

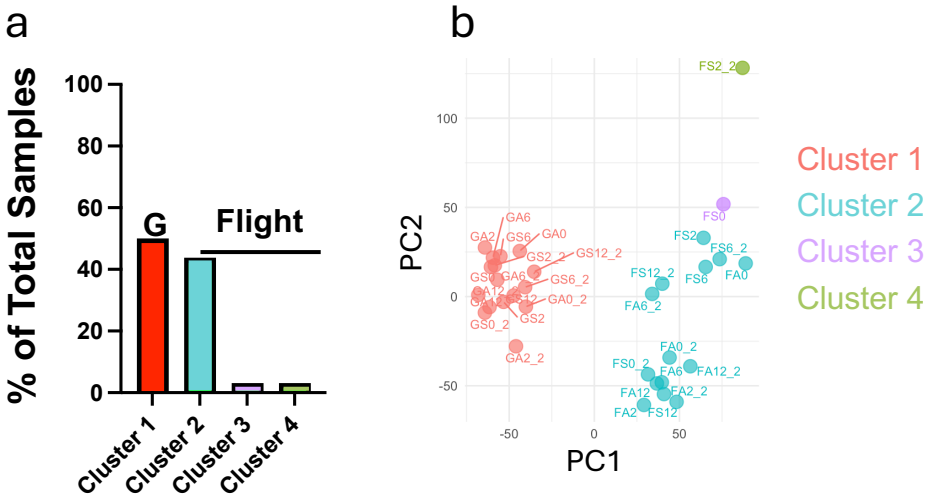

Supplemental Fig. S4. K-means clustering of spaceflight and ground control transcriptome data sets. (a) Histogram showing the proportion of the k-means clusters with four distinctive clusters including one cluster gaining the ground (G) samples and three spaceflight (Flight) clusters. (**b**) Scatter plots depicting the spatial distribution of of all RNA-seq samples on PC1 and PC2 including spaceflight (F), ground (G), aposymbiotic (A), symbiotic (S) and the individual time points (0, 2, 6, and 12 h).

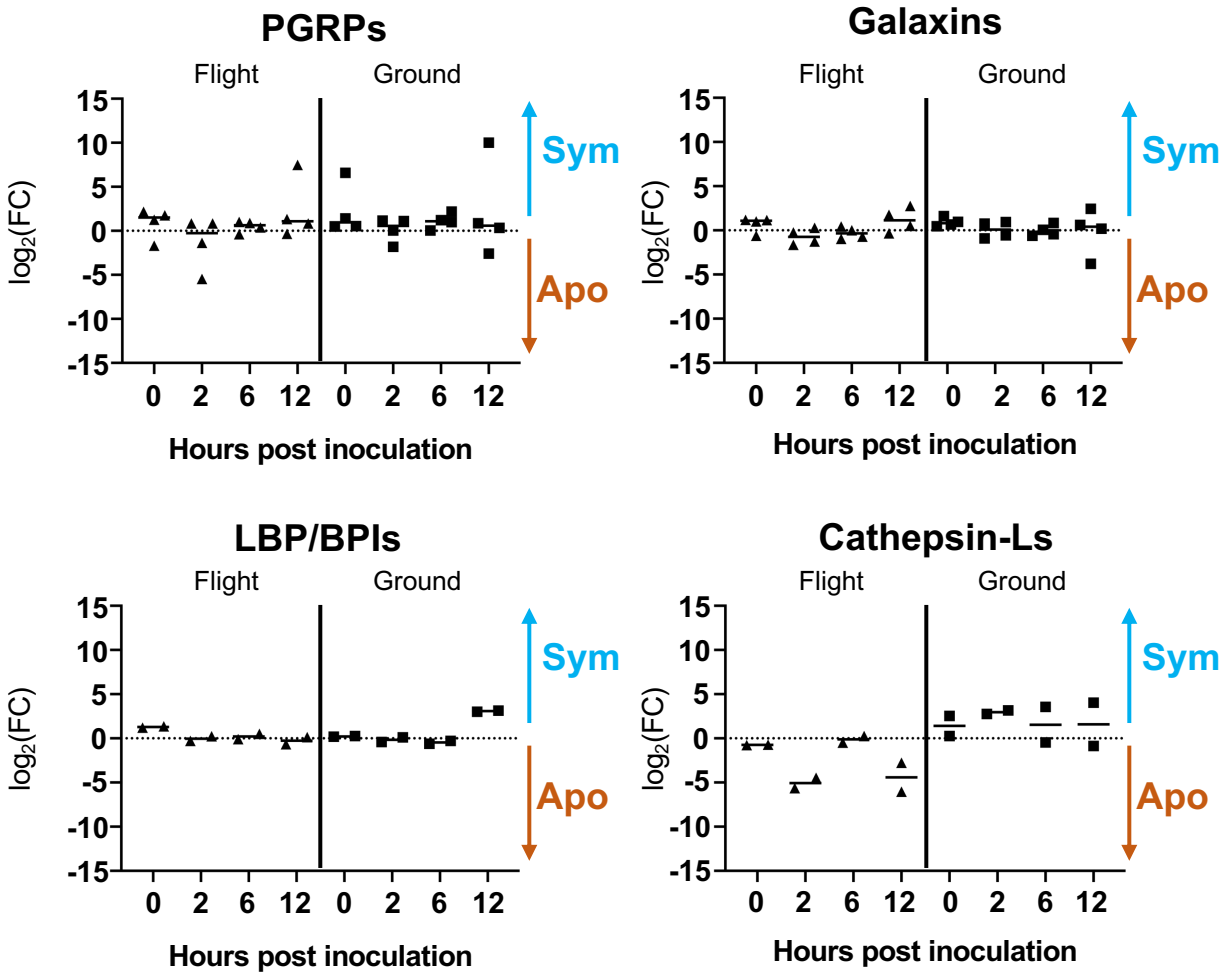

Supplemental Fig. S5. Overview of the expression of host genes typically associated with the onset of symbiosis in the squid-vibrio symbiosis. Scatter plot of genes that are typically associated with symbiont colonization including peptidoglycan receptor proteins (PGRPs), galaxins, cathepsin-L proteins and lipopolysaccharide binding proteins (LBP) under spaceflight (triangle) and ground control (square) conditions over time. Genes with a positive fold change (FC) upregulated in the presence of *V. fischeri* (sym) relative to animals maintained without symbiotic bacteria (apo). Results show few significant differences in either flight or ground controls; however, the overall trends suggest a higher expression in symbiotic animals compared to aposymbiotic animals.

a

0 h	2 h	6 h	12 h	
34 16⇧,18⇩	4 2⇧,2⇩	17 9⇧,8⇩	127 91⇧,36⇩	Ground – DEGs
5 2⇧,3⇩	48 4⇧,44⇩	29 10⇧,19⇩	39 10⇧,29⇩	Flight - DEGs

b

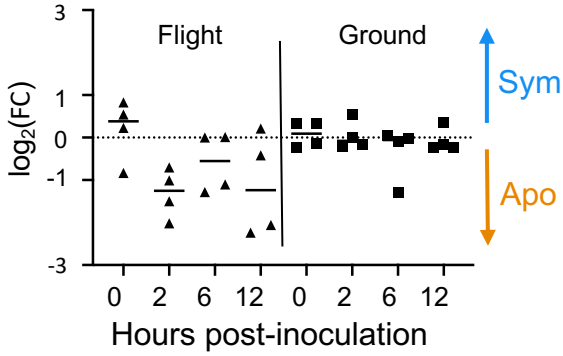

Tryptophan metabolism genes

asmbl_17118.p1	tryptophanase-like isoform X2
asmbl_14438.p1	tryptophan 2,3-dioxygenase-like
asmbl_17117.p1	tryptophanase-like isoform X2
asmbl_15742.p1	kynurenine 3-monooxygenase-like

Supplemental Fig. S6. Overview of differential gene expression during the UMAMI experiment. (a) Differentially expressed genes (DEGs) (FDR<0.1) when comparing symbiotic and aposymbiotic conditions during spaceflight (Flight) and normal gravity (Ground). At each time point, the total number of differentially expressed genes (black), genes upregulated under symbiotic conditions (blue), and genes upregulated under aposymbiotic conditions (orange) is displayed. **(b)** A scatter plot (left) of genes associated with tryptophan metabolism genes (right) over time depicting changes in gene expression in SYM (blue) relative to APO (orange) animals under flight (triangle) or ground (square) conditions. The log2-fold change (FC) calculated as SYM/APO is represented on the y-axis and the time of sampling post-inoculation is on the x-axis.

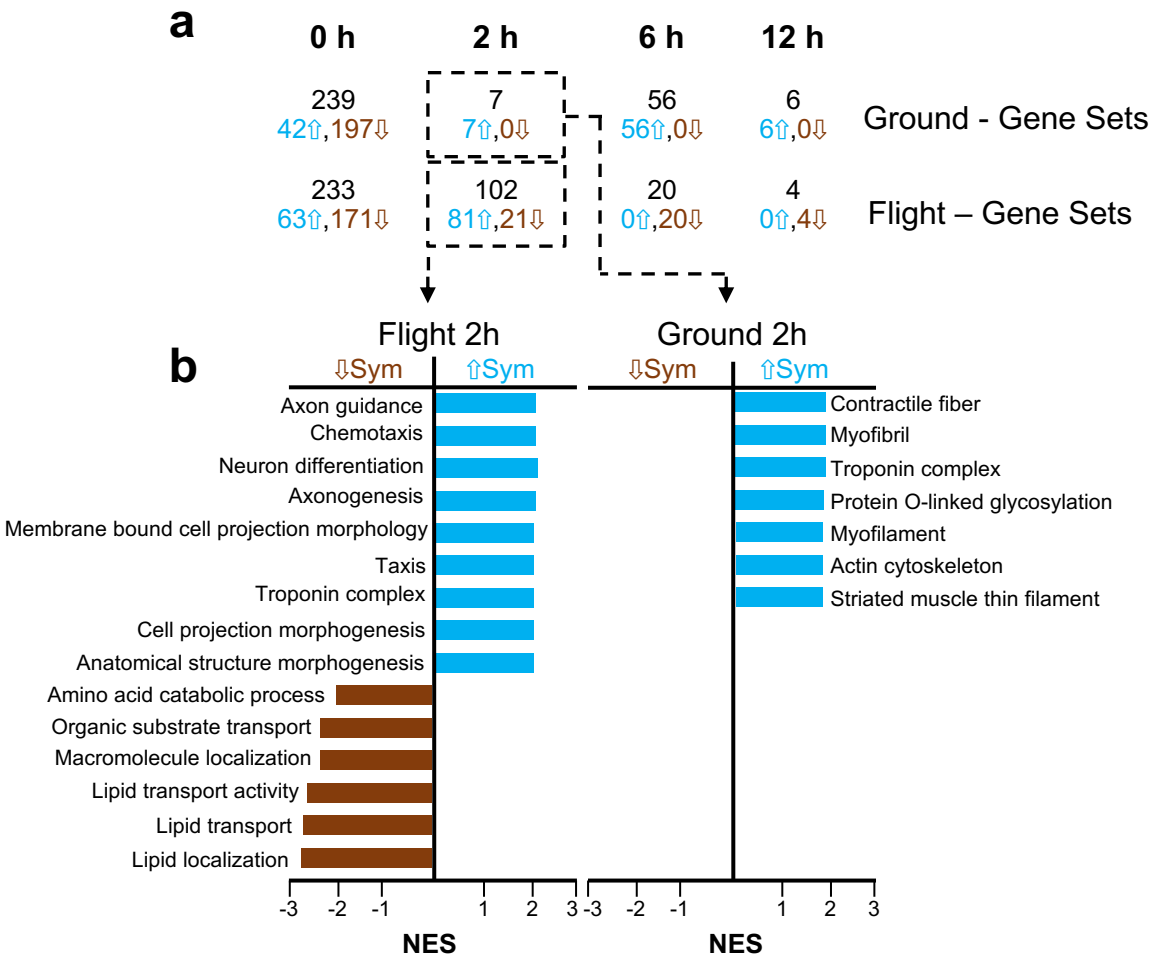

Supplemental Fig. S7. Comparison of transcriptome data from the UMAMI flight experiment. (a) Gene set enrichment (GSEA) comparisons of transcriptomes derived from ground controls and flight samples at each time point of the experiment. Total number of significant gene sets are in black. Numbers of enriched gene sets in symbiotic animals relative to aposymbiotic animals are marked in blue, whereas genes that are decreased in symbiotic animals relative to aposymbiotic animals are listed in orange. (b) Histogram of GSEA analysis comparisons at 2 h post-inoculation depicting the distinct categories that are either enriched (blue) or decreased (orange) according to the normalized enrichment score (NES) in symbiotic animals compared to aposymbiotic animals.

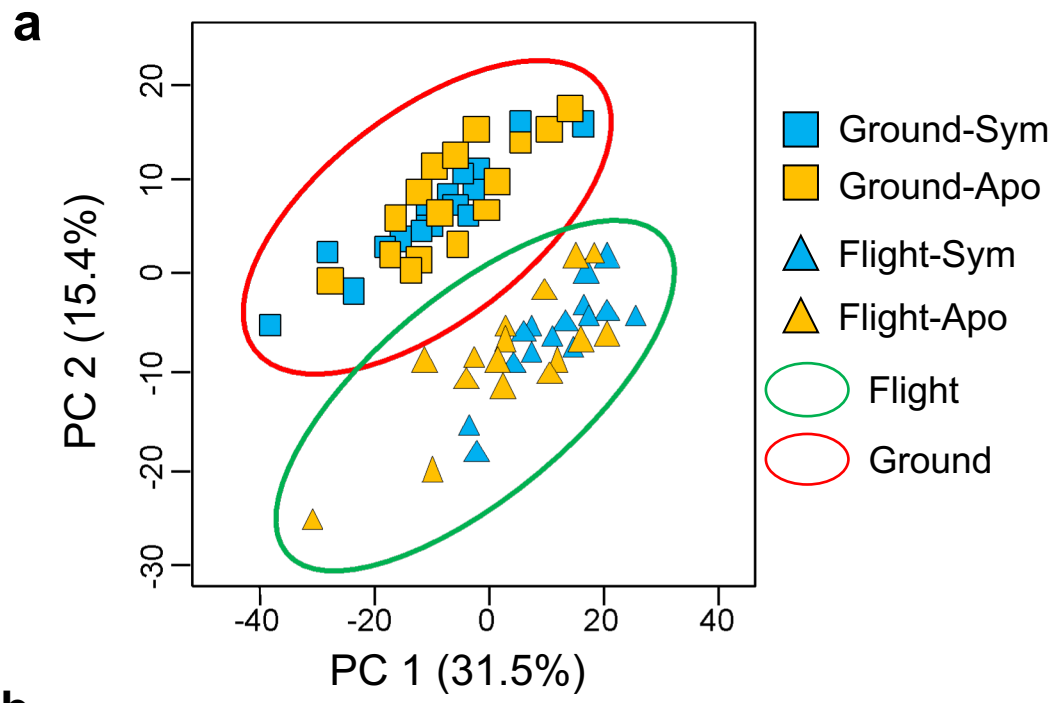

b

	0h	2h	6h	12h
Ground:	2 0⇧,2⇩	18 2⇧,16⇩	103 32⇧,71⇩	21 20⇧,1⇩
Flight:	244 68⇧,176⇩	227 140⇧,87⇩	23 17⇧,6⇩	208 162⇧,46⇩

Supplemental Fig. S8. Lipidome of host animal tissues exposed to spaceflight are distinctive from ground-based controls based on negative-ESI data. (a) Principal coordinate analysis of negative lipidomic data depicting the differences between flight (triangles) and ground controls (square). Flight animals also showed differences based on their symbiotic state with symbiotic (SYM, blue) animals forming distinctive clusters from aposymbiotic (APO, orange) animals that did not get exposed to symbiosis competent bacteria. Ellipses reflect 95% confidence that the data falls within the boundaries. **(b)** Timeline of differentially abundant metabolites at each of the timepoints examined during flight and ground controls. Upper number reflects the total number of significant metabolites ($p > 0.05$), lower numbers indicate numbers of metabolites that are either significantly up (blue) or down (orange) expressed relative to aposymbiotic animals.

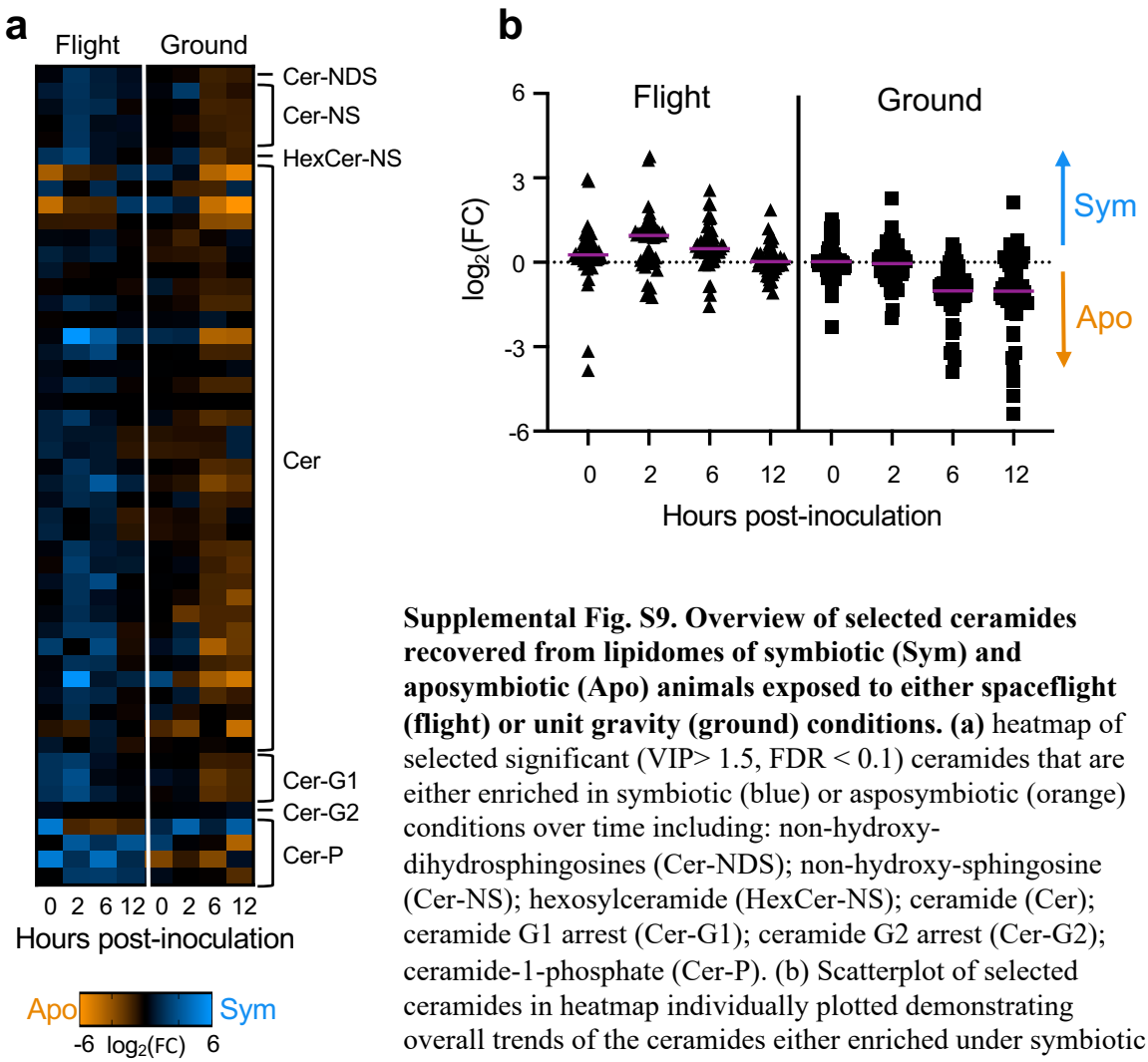

Supplemental Fig. S9. Overview of selected ceramides recovered from lipidomes of symbiotic (Sym) and aposymbiotic (Apo) animals exposed to either spaceflight (flight) or unit gravity (ground) conditions. (a) heatmap of selected significant (VIP> 1.5, FDR < 0.1) ceramides that are either enriched in symbiotic (blue) or asposymbiotic (orange) conditions over time including: non-hydroxy-dihydrosphingosines (Cer-NDS); non-hydroxy-sphingosine (Cer-NS); hexosylceramide (HexCer-NS); ceramide (Cer); ceramide G1 arrest (Cer-G1); ceramide G2 arrest (Cer-G2); ceramide-1-phosphate (Cer-P). (b) Scatterplot of selected ceramides in heatmap individually plotted demonstrating overall trends of the ceramides either enriched under symbiotic (blue) or aposymbiotic (orange) conditions. Pink bar represents the mean fold change for all ceramides for each timepoint.

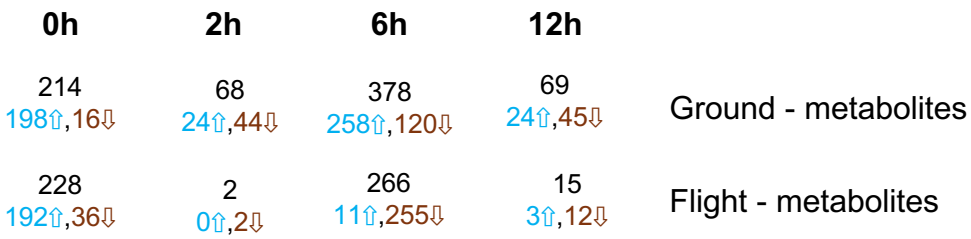

Supplemental Fig. S10. Timeline of differentially abundant metabolites under spaceflight and ground conditions based on positive electrospray ionization. For each time point, the top number reflects the total amount of significant metabolites (VIP> 1.5, FDR < 0.1) when comparing symbiotic (SYM) and aposymbiotic (APO) animals, the lower numbers indicate the number of metabolites that are either significantly increased (blue) or decreased (orange) in SYM relative to APO.

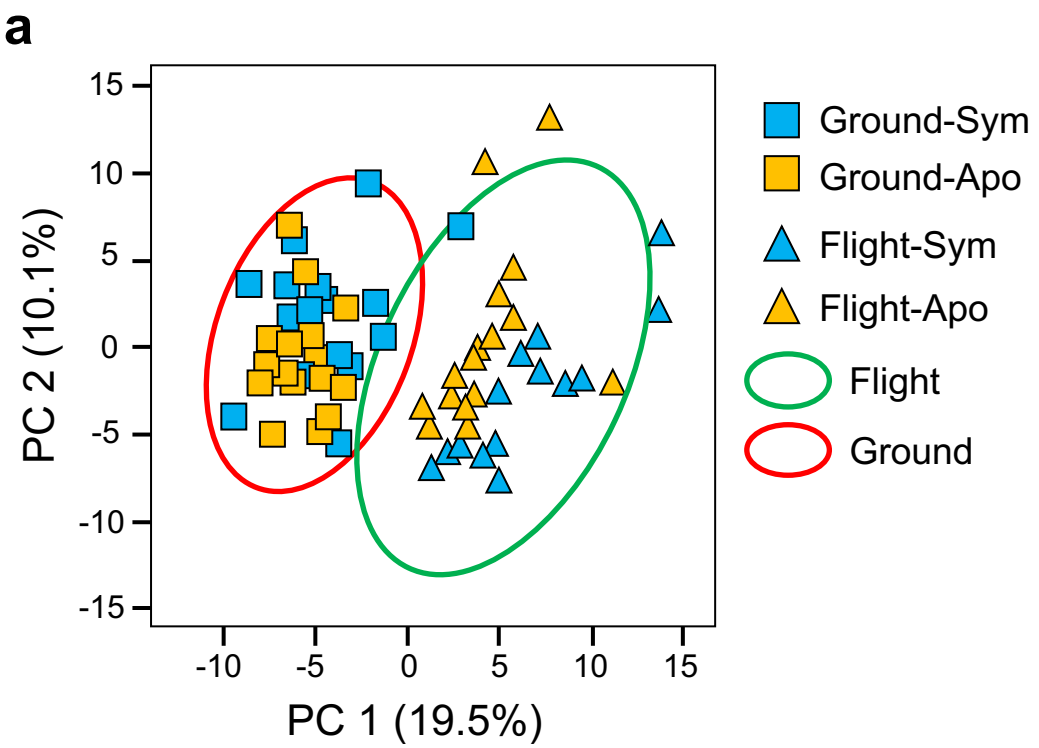

b

	0h	2h	6h	12h
Ground - metabolites	12 12⇧,0⇩	22 16⇧,6⇩	14 7⇧,7⇩	32 22⇧,10⇩
Flight - metabolites	34 8⇧,26⇩	58 5⇧,53⇩	15 0⇧,15⇩	37 0⇧,37⇩

Supplemental Fig. S11. Metabolome of host animal tissues exposed to spaceflight are distinctive from ground-based controls based on negative-ESI data. a Principal component (PC) analysis of negative metabolomic data depicting the differences between flight (triangles) and ground controls (square). Results suggest that ~20% of the variation observed between treatments can be explain in part by spaceflight conditions. Flight animals also showed differences based on their symbiotic state with symbiotic (SYM, blue) animals forming distinctive clusters from aposymbiotic (APO, orange) animals that did not get exposed to symbiosis competent bacteria. **b** Timeline of differentially abundant metabolites at each of the timepoints examined during flight and ground controls. Upper number reflects the total number of significant metabolites (VIP>1.5, FDR < 0.1), lower numbers indicate numbers of metabolites that are either significantly up (blue) or down (brown) expressed relative to aposymbiotic animals.